Original Research Article

Formation, drug-release kinetics and solution-stability of N-acetyl-N-carboxymethyl chitosan nanoparticles as potential drug carriers

Helen Priscila Bassani[1], Francine Valenga[1], Maria Rita Sierakowski[1], Rilton Alves de Freitas[1*]

*Corresponding author:

Rilton Alves de Freitas

[1]BioPol , Chemistry Department, Federal University of Paraná – UFPR, P.O. 19081, Curitiba (PR), 81531-980, Brazil.

A b s t r a c t

Nano-aggregates of N-acetyl-N-carboxymethyl chitosan (NCac) were studied at 0.5 mg.mL^{-1} using pyrene fluorimetry analysis in 0.1 mol.L^{-1} phosphate buffer (pH 7.4). The size and morphology of the aggregates were determined by dynamic light scattering and atomic force microscopy. The stability of the particles for periods up to 20 h in buffer was determined. Camptothecin was entrapped in the particles using various methods and the rate constant for drug release (k) was determined. Lower k values indicate strong interactions between the drug and the hydrophobic core of the polymeric micelles.

Keywords: N-acetyl-N-carboxymethyl chitosan; nanoaggregation; nanoparticle; light-scattering (dynamic); stability, controlled release.

Introduction

Polymers and amphiphilic co-polymers have emerged as new materials with applications in the pharmaceutical and cosmetic industries, in addition to molecular biology; they are utilized because they can form spherical micelles and capsular nanostructures [1-5]. Polymeric micelles have become attractive drug and gene delivery devices; the hydrophobic core acts as a reservoir for lipophilic drugs, while the hydrophilic surface acts as an interface between the aqueous phase and the hydrophobic core [6-8].Chitosan is a polymer used for aggregate and micelle formation. However, because it has limited solubility, different chemical modifications were developed, such as carboxymethylation, to overcome this restrictive characteristic [9-14]. The chitosan-derived polymeric micelles could be used for entrapment of hydrophobic drugs, which include taxol [15], paclitaxel [10], camptothecin [5] and 5-fluorouracil [16].

Camptothecin (CPT), which is an alkaloid from *Camptotheca acuminate,* is a potent drug used in the treatment for solid gallbladder, stomach and rectum tumors, as well as leukemia. CPT maintains an equilibrium between lactone and carboxylate forms. The lactone form of CPT is active, but because the carboxylate groups have a high affinity for albumin at physiological pH, the equilibrium rapidly shifts to favor the inactive carboxylate form [17]. The derivatization of CPT and the entrapment of the parent drug in nanostructures have become two major strategies utilized to improve lactone stability and aqueous solubility.

The use of polymeric nanoparticles may promote the delivery of CPT into tumor sites because of their small size and enhanced penetrative ability into vessels, as well as their interactions with specific parts of the human body [18,19]. Efforts to improve these particles have focused on higher drug loading, more efficient drug delivery, and resistance against both chemical and biological degradation [20,21].

We evaluated the chemical formation and acetylation of N-carboxymethyl chitosan, as well as the conditions for the nanoaggregation of the product, N-acetyl-N-carboxymethyl chitosan (NCac). Additionally, the stability of the nanoaggregates in solution, loading capacity for camptothecin, and kinetics of drug release were evaluated. Nanoaggregation of NCac could create new, stable particles in solution with the ability to encapsulate lipophilic drugs and prolong drug release.

Materials and Methods

Chitosan, N-carboxymethylchitosan, N-acetyl-N-carboxymethylchitosan and camptothecin

Chitosan from shrimp shells was obtained commercially from China (Shangyu Biotech Co., Ltd). N-carboxymethylation of chitosan (NC) (Figure. 1A) with glyoxylic acid was performed as previously described [22-24]. For every 3.5 g of chitosan added to 1 L of acetic acid (0.1 mol.L^{-1}, pH = 4.5, after 24 h of stirring), a 50% glyoxylic acid solution was added to obtain derivatives with 50% theoretical carboxymethylation. The mixtures were mechanically stirred for 24 h before the pH was adjusted to 8.0 with 0.1 mol.L^{-1} of NaOH. Subsequently, a 2% solution of NaBH$_4$ was added. The reaction was stirred for an additional 24 h. Next, the pH was adjusted to 6–8 and the system was filtered under vacuum. The filtered product (NC) was precipitated using 3 L of ethanol and dried at room temperature (25° C) under vacuum.

To re-acetylate NC, 2.0 g were dispersed in 100 mmol.L^{-1} of acetic acid (100 mL). The sample was diluted with 250 mL of methanol and a solution of acetic anhydride in methanol was added. In this work, we used 0.2 equivalents of acetic anhydride relative to N-carboxymethylchitosan because higher amounts created a material that was completely insoluble in water. After 24 hours, the polymer was precipitated with 1 L of ethanol, filtered through a nylon cloth, washed and dried under a vacuum at room temperature (25 C), which completed the formation of N-acetyl-N-carboxymethylchitosan (NCac) (Figure. 1B).

The degree of NC carboxymethylation was evaluated by both titration and by ^{1}H-NMR. A titration curve was constructed by dissolving 0.25 g of NC in 100 mL of water, bringing the solution to

~ pH 2 with 0.1 mol.L^{-1} HCl (titrated with 0.1 mol.L^{-1} NaOH). The degree of carboxymethylation determined by ^{1}H-NMR was calculated using the H2 signal proton from –CH$_2$- of glyoxylic acid and using the following equation:

$$DC(\%) = \left(\frac{H(-CH_2-)/2}{H1} \right) \times 100 \qquad \text{eq. 1}$$

Camptothecin (Figure. 1C) was obtained from Sigma-Aldrich and had a molar mass of 348.35 g.moL^{-1}, a molecular formula of $C_{20}H_{16}N_2O_4$, a pKa of 10.8 and a log P of 0.95; this information was provided by the supplier.
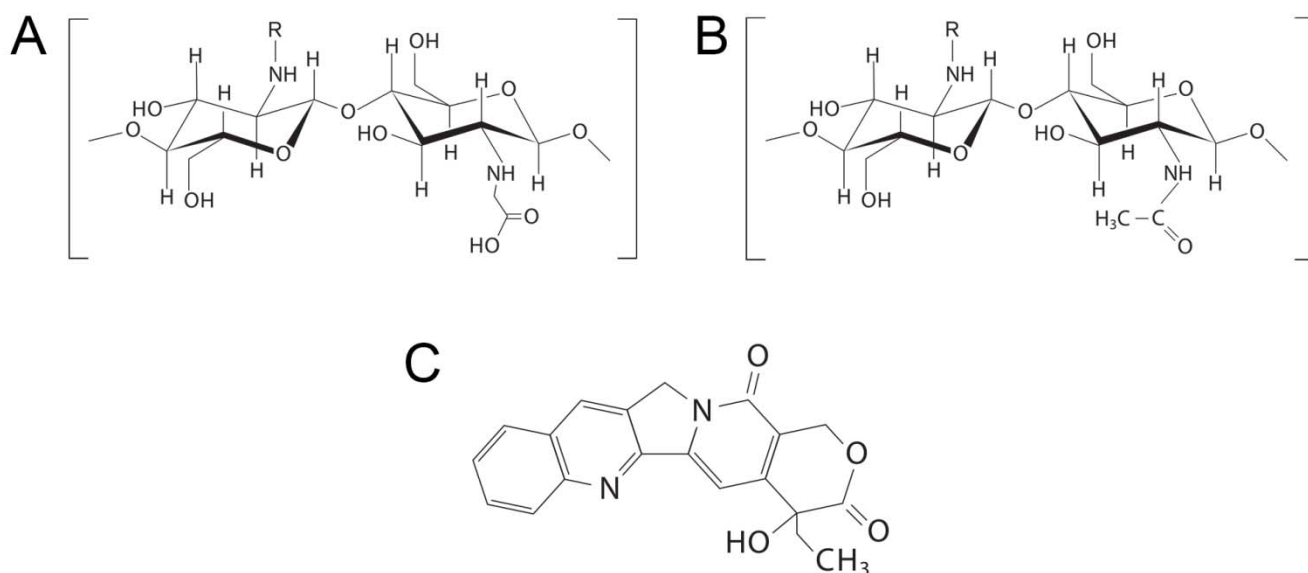

Figure 1. Schematic representation of 1A: N-carboxymethylchitosan (NC); 1B: N-acetyl-N-carboxymethylchitosan (NCac) and 1C: camptothecin.

Characterization of NCac

NCac was characterized by FTIR [25], ^{1}H and bidimensional ^{1}H-^{13}C- NMR. The FTIR analysis was performed in a Hartmann and Braumn MB-series instrument and samples were immobilized in KBr. The acquisition range for the FTIR study was 400 to 4000 cm^{-1} and the resolution was 2 cm^{-1}; samples were constructed using 2 mg of NCac and 100 mg of KBr.

^{1}H-NMR was also used to calculate the degree of acylation (DDA). The samples (10 mg.mL^{-1}) were repeatedly dissolved in D$_2$O, which resulted in complete deuterium exchange, and was then freeze-dried (3 times). ^{1}H-NMR and HMQC spectroscopic experiments were carried out using a 400 MHz Bruker model DRX Avance III NMR spectrometer, which incorporated a Fourier transform and used a 5 mm inverse gradient probe. Spectra were obtained at 80 C and the chemical shifts are expressed in ppm ( ).

The DDA calculation from the ^{1}H-NMR spectral data were determined using two different methods. The first method was based on the work of Hirai, Odani, and Nakajima [26]; the signal protons H2, H3, H4, H5, H6 and H6 from NCac were used in equation 2, below. The second method was based on the work of Lavertu [27]; the integrals of the proton H1 peak from a deacetylated monomer (H1D) and the peak from the acetyl group, which accounted for three protons (HAc), were used in equation 3, below.

$$DDA(\%) = \left(1 - \left(\frac{1}{3} HAc \middle/ \frac{1}{6} H2 + H3 + H4 + H5 + H6 \right) \right) \times 100 \qquad \text{eq. 2}$$

$$DDA(\%) = \left(\frac{H1D}{H1D + HAc/3} \right) \times 100 \qquad \text{eq. 3}$$

Stability studies of NCac by TDLS in different solvents

Stability studies of NCac were performed by continuous measurement of dynamic light scattering at 90º, which was performed in NanoDLS equipment from Brookhaven Instruments Corporation. The raw voltage from the detector was used to measure the sample stability over 20 h at 25 C. Time dependence light scattering (TDLS) used 0.1 mol.L^{-1} phosphate buffer (pH 7.4) and a sample of NCac at 1 mg.mL^{-1}.

Polymeric molar mass determination

For the GPC analysis, the experiments were carried out at 30 C in a Viscotek GPC Multi-detector. Refractive index (RI), light scattering (LS) and Malvern viscometer systems, which used an 806HQ Shodex-OH pack column, were utilized in this experiment. The samples of NC and NCac (1 mg.mL^{-1}) were solubilized in aqueous 0.1 mol.L^{-1} Tris-HCl buffer (pH 8.2), which contained 0.02% (w/w) sodium azide, and filtered through a 0.45 µm pore-diameter membrane, as previously described [14].

Surface tension studies and fluorescence assay

The critical concentration for the aggregation of NCac was determined using concentrations from 1.0 x 10^{-2} to 5.0 mg.mL^{-1} in 0.1 mol.L^{-1} phosphate buffer (pH 7.4). The surface-tension measurements were performed at 25 C using a DataPhysics OCA15 plus tensiometer. The fluorescence assays, which used pyrene as a hydrophobic marker, were performed at a final concentration of 2 µmol.L^{-1}, in addition to the same concentration of polymer used in the surface-tension measurements. The pyrene experiments used an excitation wavelength of 343 nm and emission wavelengths ranging from 360 to 500 nm; measurements were taken using a Hitachi F-4500 Fluorescence Spectrophotomer. The changes in vibratory bands I and III, which were at 373 and 384 nm, respectively, were evaluated to understand the hydrophobic domains in the polymer [28].

Characterization of NCac particles

NCac samples at both 1 mg.mL^{-1} and 5 mg.mL^{-1} were evaluated in 0.1 mol.L^{-1} phosphate buffer (pH 7.4) at temperatures ranging from 25 to 75 C, which were separated by increments of 5 C. Colloidal stability, which was obtained as a function of temperature, was determined using NanoDLS equipment from Brookhaven Instruments Corporation.

Topographical analyses were performed using a 5500 Agilent PicoPlus molecular imager in tapping-mode, which utilized a NSC14 silicon cantilever with a spring constant of 5 N.m^{-1} a and resonance frequency of 182 Hz. The data were analyzed using SPIP^{TM}, Scanning Probe Image Processor software.

Entrapment efficiency for camptothecin in NCac particles.

CPT was incorporated into NCac using three different methods. The parent polymer NC exhibited a low capacity for drug-loading in preliminary studies and was not studied further. The equilibrium solubility of CPT in the absence and presence of the polymer was tested over the 72 h, which began after dispersion, in aqueous media. The three procedures for drug loading were:

Method 1: The first method entailed the co-dispersion of 200 µg.mL^{-1} CPT and 1000 µg.mL^{-1} NCac in 0.1 mol.L^{-1} phosphate buffer (pH 7.4).

Method 2: A 1000 µg sample of CPT was solubilized in 1 mL chloroform and 0.7 mL acetonitrile. Next, 5000 µg of NCac was dispersed in this solution. The organic solvent was evaporated using a stream of nitrogen. Subsequently, 5 mL phosphate buffer (0.1 mol.L^{-1}, pH 7.4) was added to the film and the sample was sonicated for 15 min.

Method 3: Samples of 1000 µg CPT and 5000 µg NCac were co-dispersed in 2 mL DMSO and subsequently dialyzed against 0.1 mol.L^{-1} phosphate buffer (pH 7.4); the volume was adjusted to 5 mL with the buffer.

Free camptothecin was removed from the camptothecin entrapped in NCac nanoaggregates by centrifuging the samples (1,000 g), which worked by separating of the dispersed polymer/drug complex from the insoluble drug.

The CPT entrapment efficiency (E) in NCac was calculated using the following equation:

$$E\% = \left[\left(\frac{CPT_{total} - CPT_{Free}}{CPT_{total}} \right) \times 100 \right] \qquad \text{eq. 4}$$

where CPT_{total} is the total concentration of CPT and CPT_{Free} is the free, insoluble camptothecin. CPT is insoluble in water, but the nanoaggregates of the NCac /CPT complex maintain a stable, colloidal dispersion in PBS buffer.

The determination of the drug entrapment efficiency was performed using reverse-phase high-performance liquid chromatography. The chromatographic resolution was achieved on a Supelcosil LC-18 column (15 cm x 4.6 mm id, 5 µm) using methanol and 10 mmol.L^{-1} KH_2PO_4 (60 + 40, v/v; pH 2.8) as the mobile phase, which had a flow rate of 1.0 mL.min^{-1}; ultraviolet detection was carried out at 254 nm [29]. The calibration curve, which had a correlation coefficient of 0.999, was linear from 0.5 to 10.0 µg.mL^{-1} and the limits of quantitation (LQ) and determination (LD) were 0.25 and 0.07 µg.mL^{-1}, respectively.

Kinetic studies of the drug release from particles

In vitro studies of the release of CPT from the nanoparticles were performed using a cellulose ester dialysis membrane (6,000-8,000 MWCO) from Spectrum Labs (Rancho Dominguez, CA), which was 20 mm in diameter and previously wetted for 12 hours with the dissolution medium (0.1 mol.L^{-1} phosphate buffer (pH 7.4 or pH 6.4), with 20% (v/v) of DMSO). Free CPT (200 µg.mL^{-1}) in the dissolution medium, or nanoparticles in colloidal dispersion, which

were effectively at a concentration of 200 µg.mL^{-1} of CPT, were placed on a dialysis membrane.

First order kinetics was applied as a model for drug release, as shown in equation 5:

$$\text{Drug}(\%) = \text{Drug}(\%)_f - \text{Drug}(\%)_0(1-\exp(-kt))$$

(eq. 5)

where Drug(%)$_f$ is the final concentration in the medium, Drug (%)$_0$ is the initial concentration in the medium, k is the drug release constant, and t is the time.

The membrane was affixed in a 250 mL Erlenmeyer flask containing 100 mL of the dissolution medium; this system was placed in a shaker with a rotation of 100 rpm at 37 C. Samples (2 mL) were withdrawn at 0, 2, 4, 6, 8, 10, 12 and 15 hours and dissolution medium was added to replace the lost volume. CPT concentrations were determined by fluorescence spectroscopy, which utilized with excitation at 360 nm, emission at 465 nm and linearity from 7x10^{-3} to 7x10^{-2} mg.mL^{-1} (R 0.99); these experiments were performed using an F-4500 Fluorescence Spectrophotomer manufactured by Hitachi.

Results and discussion

Preparation and characterization of N-carboxymethylated and acetylated derivatives

NC and NCac were prepared and characterized as previously described [13]. As shown by the alkalimetric curve, NC exhibits 50% carboxymethylation; its structure was initially compared with the structure of NCac by FTIR analysis.

Characteristic absorption peaks were observed at 3000-4000 cm^{-1} (-OH) and at 1750 cm^{-1} (C=O of the –COOH group) for both NC and NCac. The absorption peaks at 1650 cm^{-1} were assigned to the carbonyl stretch of the secondary amides (amide I band); the N–H bending vibration of the non-acylated 2-aminoglucose primary amines at 1570 cm^{-1} was clearly less prominent in the NCac sample. The acetyl group was observed at 2920 and 2870 cm^{-1} (C-H stretching) and was a stronger signal in the N-acetylate sample (NCac) (data not shown).

Table 1. Acetate free and N-acetyl determined by ^{1}H NMR and Carboxymethyl group (%) using titration and ^{1}H-NMR.

Sample	Carboxymethyl group (%)		Acetyl group (%)				
	Titration	^{1}H-NMR	Free ^{1}H-NMR		N-acetyl ^{1}H-NMR		Total (free+N-acetyl) ^{1}H-NMR
			Eq. 2	Eq.3	Eq. 2	Eq. 3	
NC	50	44.2	12.5	17.0	3.0	3.5	18.0
NCac	-	42.4	11.3	15.2	15.6	22.1	32.1

.

The structures of NC and NCac were also confirmed by ^{1}H and ^{1}H-^{13}C NMR (Figure. 2) experiments. The evaluations of the carboxymethylation and DDA for both NC and NCac were based on ^{1}H-NMR and calculated using equations 1, 2 and 3. The values for the carboxymethyl, free acetyl and N-acetyl experiments are shown in Table 1.

The extent of carboxymethylation in NC and NCac were 44.2 and 42.4%, respectively, by ^{1}H-NMR and 50% by titration. The average values of total acetylation were similar in the FTIR and ^{1}H-NMR data, with 30.0% and 32.1% acetylation, respectively; this result indicates that only 20% of the free amine groups persisted in the structure of NCac. However, quantitative ^{1}H-NMR studies of the acetyl groups revealed two different forms. The ionically bound acetate on the amine group accounted for 11.3 to 15.2% (free acetyl) and the covalently bound N-acetyl groups accounted for 15.6 to 22.1%; these values were determined using equation 2 and 3, respectively.

The structural modifications introduced by the re-acetylation of NCac are reflected in the HMQC spectra. The carbon and the hydrogen peaks are identified in Fig. 2C. The main difference between NC and NCac is the presence of N-acetyl groups, which

are denoted by the signals at 2.41 and 24.5 in the ^{1}H and ^{13}C-NMR spectra, respectively. The NC sample, which is a fully deacetylated sample (from 3.0% to 3.5% of N-acetyl groups), exhibits 12.5 to 17.0% ionically bound acetate.

The NCac spectra present a more intense N-acetyl peak at these chemical shifts, which is because the acetylation occurs mostly at the free amine site on C-2. The identity of the peak at 2.5, which was assigned to the ionically bound acetyl groups, was confirmed by doping both solutions with 0.052 mmol of acetic acid (data not shown) and subsequently observing a considerable increase in this peak's intensity [27].

All observed peaks could be correlated with those published previously [13, 30] and are exhibited in Figure. 2. These peak data confirmed the presence of N-carboxymethylation, which was the expected result of the reaction between glyoxylic acid and chitosan. The acetylation, which was carried out using acetic anhydride in methanol, promoted the reaction on the remaining amine groups in NC.

This acetylation reaction involves the nucleophilic addition of an un-protonated primary amine, which is from glucosamine, to acetic anhydride. Since acetic anhydride is readily hydrolyzed by water,
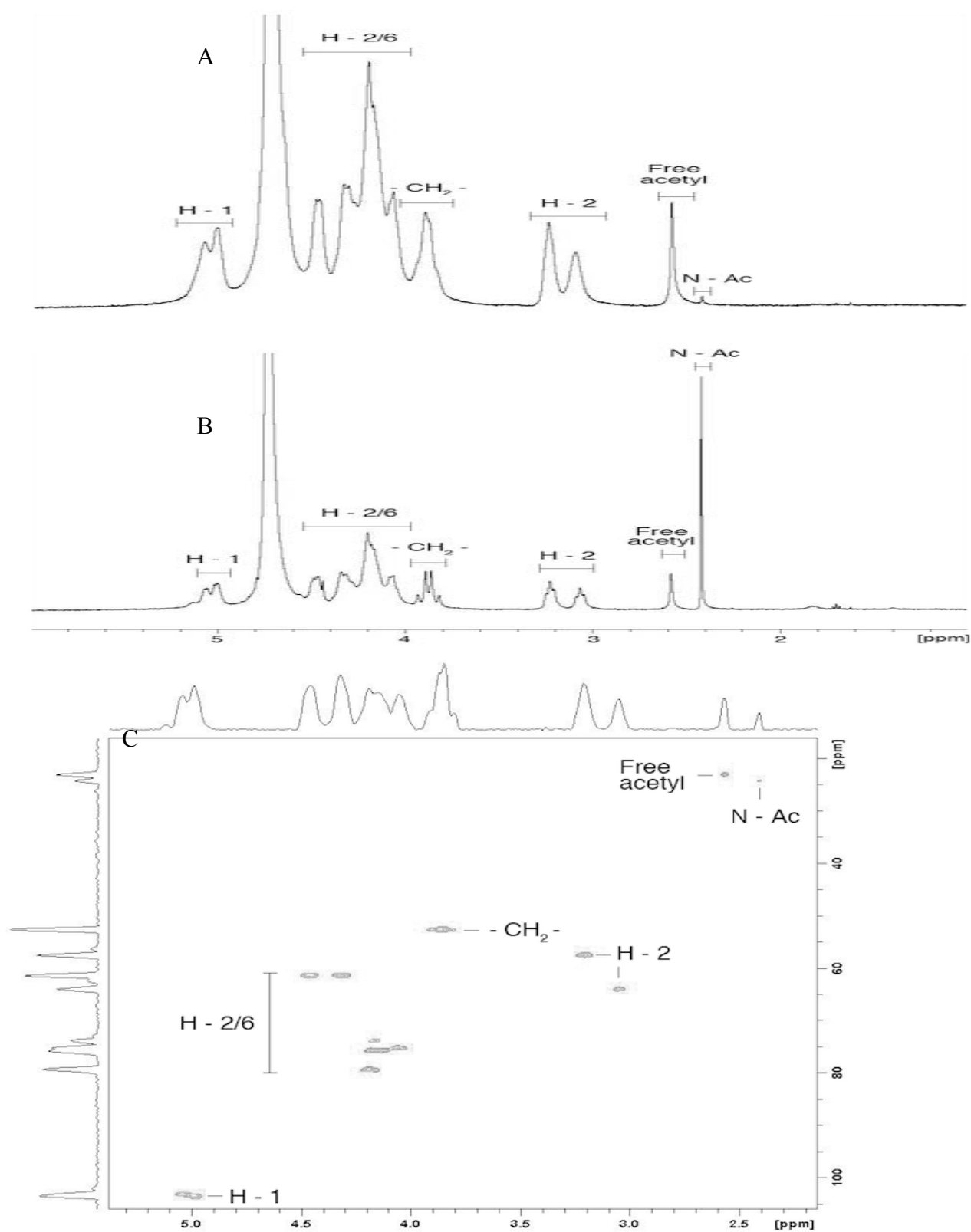
Figure 2. ¹H-NMR spectra of N-carboxymethylchitosan (NC) (A), N-acetyl-N-carboxymethylchitosan (NCac) (B) and ¹H-¹³C NMR correlations of NCac (C) in D₂O, at 80 °C.

mixtures of methanol (MeOH) and water are typically used as the solvent when reacetylating chitosan. It is also known that chitosan is not soluble in 100% MeOH; therefore, the reaction could not be performed under conditions precluding the hydrolysis of acetic anhydride [31].

The acetylation of N-carboxymethylchitosan creates a hydrophobic core in the polymer structure, which will be evaluated below, and can consequently be used to carry relatively water-insoluble compounds, such as CPT.

Stability of derivatives in different buffers and pH's

N-acetyl-N-carboxymethylchitosan (NCac) demonstrated less aggregation and macromolecular behavior in alkaline buffer (pH 8.2); this effect was due to the ionization of N-carboxymethyl group, which promoted electrostatic repulsion between the acid groups and generated more favorable conditions for polymer-solvent interactions (Figure. 3).
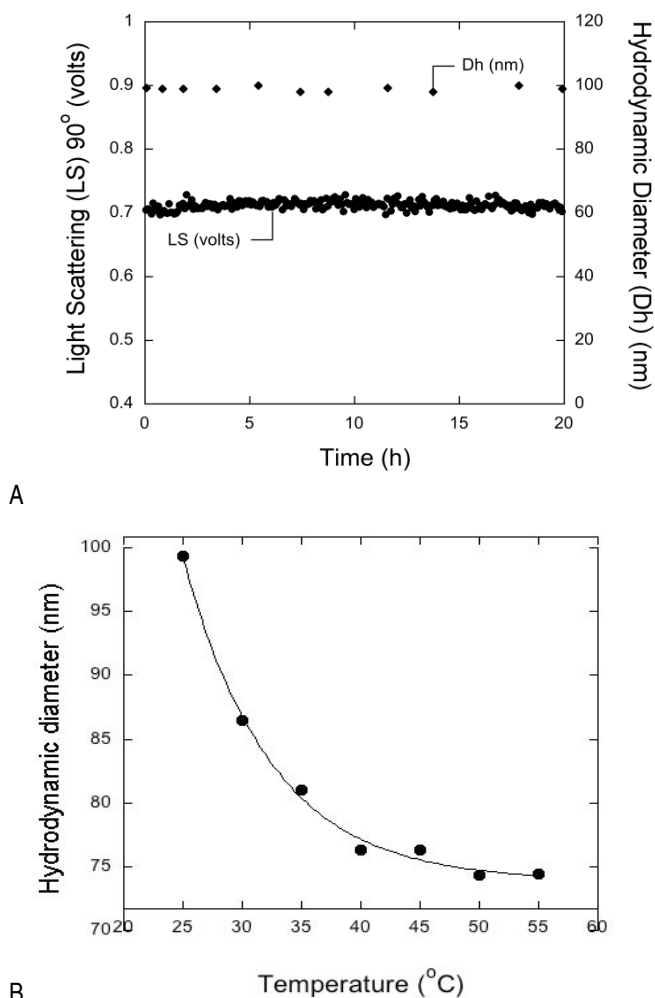

A

B

Figure 3. (A) Stability of NCac by TDLS using pH 7.4 at 25°C. (B) Dynamic light scattering (D_h) of NCac in 0.1 mol.L^{-1} phosphate buffer pH 7.4 as a function of the temperature.

Table 2. GPC results and chemical quantifications for NC and NCac in 0.1 mol.L^{-1} Tris-HCl pH 8.2.

Sample	NC	NCac
$M_w/10^{-5}$ g.moL^{-1}	2.29	3.03
$M_n/10^{-5}$ g.moL^{-1}	0.230	0.362
$M_{peak}/10^{-5}$ g.moL^{-1}	0.283	0.378
M_w/M_n	9.9	8.3
IV (dL.g^{-1})	0.297	0.370

Samples of NC and NCac, which were dispersed in 0.1 mol.L^{-1} Tris-HCl buffer (pH 8.2), were used to study the systems' macromolecular properties (Table 2). GPC analysis indicated that polydispersed samples (M_w/M_n from 9.9 to 8.3) had an intrinsic viscosity of 0.297 and 0.370 dL.g^{-1} and an M_w of 2.29 x 10^5 g.moL^{-1} and 3.03 x 10^5 g.moL^{-1}, respectively, for NC and NCac.

Additionally, at pH 7.4, the equilibrium between carboxylic acid moieties and the buffer's phosphate groups was strongly influenced by the free amino groups; this perturbation of the equilibrium considerably diminished the favorable interactions with the solvent, which induced the formation of aggregates.

The stability of the NCac aggregates was studied with a light scattering signal at 90 (Figure. 3A) in 0.1 molL^{-1} phosphate buffer (pH 7.4). The aggregates were stable for up to 20 h of analysis, which suggested that NCac would be a good candidate for drug entrapment and delivery. The hydrodynamic diameter (D_h) was also constant under these pH and temperature conditions (Fig. 3A). Particles with hydrodynamic diameters (D_h) at 99.2 and 74.4 nm, at 25 C and 55 C, respectively, were analyzed by DLS (Fig. 3B); the nanoparticles were influenced by the temperature and the aggregates increased in size when the temperature rose.

The morphology of the nanoparticles (Figure. 4) was analyzed using atomic force microscopy (AFM). The AFM analysis showed spherical particles, which had a mean diameter of 80.85 ± 18.50 nm (n=30), deposited on mica at 25 C. The dimensions measured by AFM were similar to the D_h obtained by DLS analysis.

According to Philippova et al [32], the nano-aggregation of chitin and chitosan is subject to 3 major parameters: 1) aggregation of chitosan derivatives modulated by hydrogen bonds; 2) crystallization of junction zones between different macromolecules, which make some hydrogen bonds inaccessible to urea or too stable to be broken; 3) strong hydrophobic bonds.

Using the pyrene peak ratio, the aggregation in solution was determined to be 0.5 mgmL^{-1}; it was observed that an increase in the concentration could saturate the water-air interface, which is a behavior common to surfactants, and micelle-like structures were observed near 3.5 mg.mL^{-1} (Figure. 5).   Aggregates are formed at lower concentrations of phosphate buffer and accumulate as the concentration rises to form micelles (accumulation of nanoaggregates). The reason that the results of the pyrene-fluorimetry and tensiometry aggregation studies differed for NCac was that the techniques were based upon different principles. The pyrene-based experiments measured the formation of aggregates
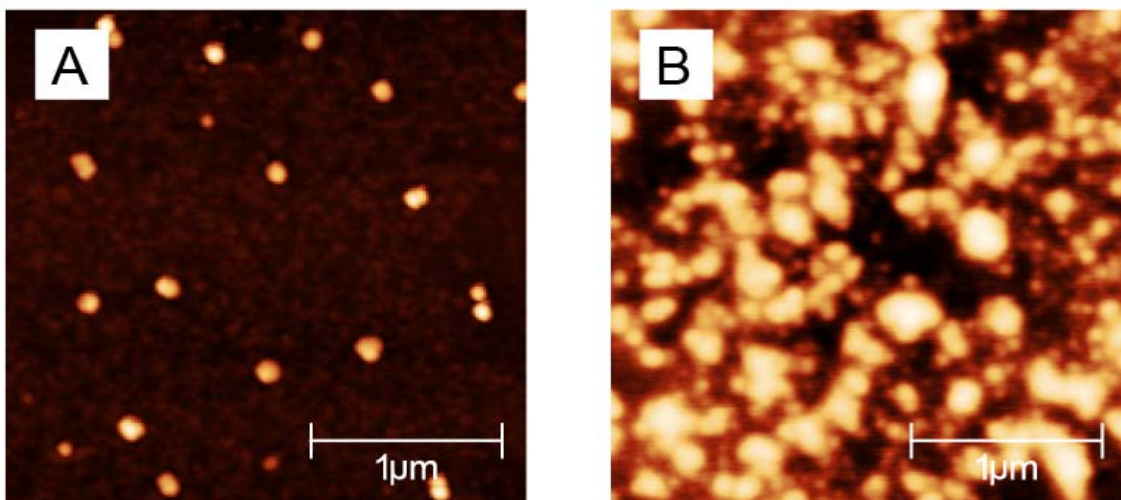
Figure 4. AFM images of NCac at 2.5x2.5 µm and insert: 1.0x1.0 µm, using Mica as support. The samples were prepared using 1mg.mL^{-1} NCac in 0.1 mol.L^{-1} phosphate saline buffer, pH 7.4.

in solution, which were promoted by the intra and intermolecular hydrogen and electrostatic bonds between the NCac chains; this effect generates hydrophobic micro-domains in solution. As the NCac concentration was further increased, the hydrophobic interactions became stronger because acetyl groups were present in the chain of NCac and the polarity of the groups available for interaction was reduced [33]. Consequently, a second feature in the pyrene curve was observed, which was accompanied by a significant reduction in the superficial tension (Figure. 5).
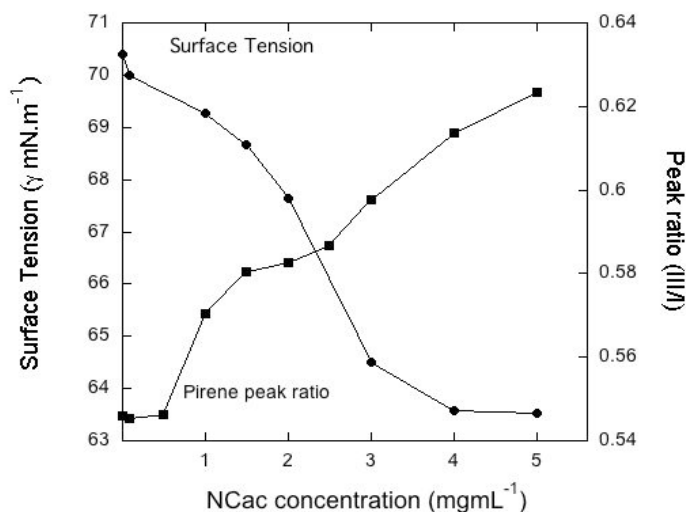

Figure 5. Surface tension (mN/m) and pyrene peak ratio (III/I) by fluorescence analysis of NCac in 0.1 mol.L^{-1} phosphate buffer pH 7.4.

Inter-particle aggregate formation, which was more prevalent in CAC than NCac solutions, was also confirmed by AFM imaging (Figure. 4B). At the concentration necessary to perform this type of imaging, it was no longer possible to observe isolated particles; only larger masses formed by the assembly of many NCac aggregates were visible.

Incorporation of camptothecin and quantification of drug content.

The therapeutic application of CPT is limited by its low water solubility, high toxicity and rapid inactivation (lactone ring hydrolysis) at physiological pH. The lactone hydrolysis, which is reversible in acidic media, leads to a water-soluble carboxylate. However, the carboxylate form is inactive and readily binds to human serum albumin, which prevents cellular uptake [34].
Methods 1, 2 and 3 increased the amount of CPT entrapped in the NCac particles (Table 3). The efficiency of CPT incorporation approached 26% and depended on the encapsulation method, which suggested that the solubility of the drug was improved by the NCac nanoparticles. The co-dispersion of CPT with only the polymer did not promote a significant increase in the drug solubility.

Table 3. CPT-loading in NCac by different methods, efficiency of drug entrapment and the rate constant (k) for release.

Samples	Loaded CPT (µg.mL^{-1})*	Efficiency (%)	k (h^{-1})
CPT	2.4±0.0	1.0	0.09
Method 1	4.7±0.5	2.3	-
Method 2	52.0±10.0	26.0	0.01
Method 3	57.6±8.5	28.8	0.02

* Using 1 mg/mL of polymer and 200 µg.mL^{-1} of CPT in all the methods.

If CPT interacts more favorably with the hydrophobic polymer chain than with the solvent, the incorporation efficiency will be high, but if CPT interacts more significantly with itself, a CPT precipitate will be formed [5]. For this work, the ratio of CPT: polymer was 1:5; lower CPT content facilitated an increase in the drug loading, which was optimal at this proportion. An increase in the concentration did not positively influence the efficiency of CPT incorporation (data not shown). Mu, Elbayoumi, and Torchilin [35] used a more complex system of polymeric micelles; they utilized a mixture of polyethyleneglicol, phosphatidylethanolamine and succinate tocopherol polietilenglicol and loaded only 30 ± 2 μg of the CPT per mL of suspension. Generally, loading CPT into NCac was more effective than this or any other previously reported systems [11,35-37]

Drug release

Kinetic studies of the release of CPT from NCac particles were enacted with samples produced by method 2 and 3 of drug-encapsulation (Figure. 6). Method 1 was not used because of its low incorporation of CPT. Identical amounts of CPT were used in each encapsulation methodology to quantify the kinetics of CPT release. Comparatively, the rate constant k (h^{-1}) for un-chaperoned CPT release was 9.4×10^{-2}; 1.6×10^{-2} and 2.0×10^{-2} were calculated for method 2 and 3 of entrapment, respectively, which resulted in k values up to 5.9 times lower (Table 3). These results confirm that CPT was incorporated into the particles instead of being superficial adsorbed to colloidal particle interfaces. In all cases, the R obtained was 0.99, which suggested that a first order kinetic model of drug release could be applied to this system.
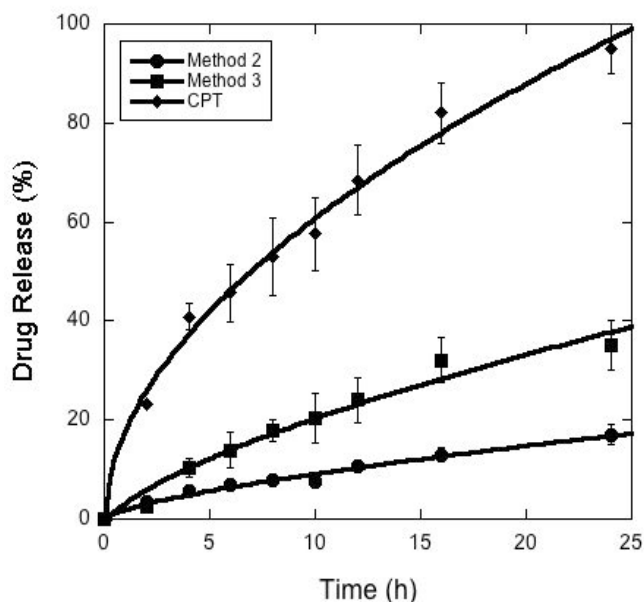

Figure 6. Kinetics of camptothecin (CPT) release from NCac, incorporated using two method 2, co-dispersing in DMSO and method 3, film formation. The nude CPT was used as reference.

Opanosopit et al. [5] proposed that the weak interactions between a drug and the inner core of the encapsulating particles partially contribute to faster drug release. This author disclosed that increasing the amount of deacetylation to 85% promoted a slower release, while less acetylation promoted faster release. Additionally, the hydrophobic core of the nanoaggregates could facilitate a crystalline structure that includes CPT, which also justifies the slow release of the drug from the aggregates [38].

Several problems, such as recognition by the host immune system, occur when the blood-circulation times for particles become long. However, the use of biopolymeric particles such as NCac could improve biocompatibility and reduce unspecific phagocytosis. The slower kinetics of the drug delivery combined with the small size (<100 nm) of the NCac particles provide an interesting approach to solid tumor treatment; the particles could survive for long periods of time in the blood stream and undergo slow deposition in the tumor sites. Solid tumors have leaky vasculature and poor lymphatic drainage, which should enhance the permeation and the retention effects [21].

Because tumor sites are also known to be acidic and the particles demonstrated less aggregation in acidic media, the drug should be released preferentially into the desired locations. Our preliminary results indicate that a reduction the pH from 7.4 (normal) to 6.4, which is the pH of tumor sites, increases the release of CPT up to 41.3% (data not shown).

Conclusion

NCac forms concentration-dependent structures that include nanoaggregates and micelle-like structures; this derivative is a good candidate for carrying hydrophobic drugs such as camptothecin because the nanoparticles are formed at relatively low concentrations, are stable for up to 20 h under physiological conditions (phosphate buffer pH 7.4), and can achieve a drug loading efficiency of 26%. A modified kinetic pathway for drug delivery was promoted, which made the release of CPT from the particles less effective.

Authors' contributions

HPB: have made substantial contributions to acquisition of data;
FV: have made contribuitions to AFM acquisition of data and interpretation of this results;
MRS: Analysis and revising it critically for important intellectual content;
RAF: have made substantial contributions to conception and design, or acquisition of data, or analysis and interpretation of data; have been involved in drafting the manuscript or revising it critically for important intellectual content; and have given final approval of the version to be published.

Acknowledgments

References

[1]. Kataoka K, Kwon G, Yokoyama M, Okano T, Sakurai Y. Block copolymer micelles as vehicles for drug delivery. J Control Release. 1993; 24: 119–132.

[2]. Kataoka K, Harada A, Nagasaki Y. Block copolymer micelles for drug delivery: design, characterization and biological significance. Adv Drug Deliv Rev. 2001; 47: 113–131.

[3]. Kwon G, Okano T. Polymeric micelles as new drug carriers. Adv Drug Deliv Rev. 1996; 21: 107-116.

[4]. Aliabadi HM, Lavasanifar A. Polymeric micelles for drug delivery. Expert Opin Drug Deliv. 2006; 3: 139–162.

[5]. Opanasopit P, Ngawhirunpat T, Chaidedgumjorn A, Rojanarata T, Apirakaramwong A, Phonggyng S, Choochottiros C, Chirachanchai S. Incorporation of camptothecin into N-phthaloyl chitosan-g-mPEG self-assembly micellar system. Eur J Pharm Biopharm. 2006; 64: 269-276.

[6]. Huh KM, Lee SC, Cho YM, Lee J, Jeong JH, Park K. Hydrotropic polymer micelle system for delivery of paclitaxel. J Control Release. 2005; 101: 59–68.

[7]. Van Nostrum CV. Polymeric micelles to deliver photosensitizers for photodynamic therapy. Adv Drug Deliv Rev. 2004; 56: 9-16.

[8]. Hruby M, Konak C, Ulbrich K. Polymeric micellar pH-sensitive drug delivery system for doxorubicin. J Control Release. 2005; 103: 137-148.

[9]. Li Q, Dunn ET, Grandmaison EW, Goosen MFA. Applications and properties of chitosan. J Bioact. Compat. Polym. 1992; 7: 370-397.

[10]. Zhang C, Qineng P, Zhang H. Self-assembly and characterization of paclitaxel-loaded N-octyl-O-sulfate chitosan micellar system. Coll Surf B. 2004; 39: 69–75.

[11]. Zhu A, Liu J, Ye W. Effective loading and controlled release of camptothecin by O-carboxymethylchitosan aggregates. Carbohydr Polym. 2006; 63: 89-96.

[12]. Zhu A, Dai S, Li L, Zhao F. Salt effects on aggregation of O carboxymethylchitosan in aqueous solution. Coll Surf B. 2006; 47: 20-28.

[13]. Felicio SGF, Sierakowski MR, Petkowicz CLO, Silveira JLM, Lubambo AF, Freitas RA. Spherical aggregates obtained from N-carboxymethylation and acetylation of chitosan. Coll Polym Sci. 2008; 286: 1387-1394.

[14]. Freitas RA, Drenski MF, Alb AM, Reed WF. Characterization of stability, aggregation, and equilibrium properties of modified natural products; The case of carboxymethylated chitosans. Mat Sci Eng C. 2010; 30: 34-41.

[15]. Miwa A, Ishibe A, Nakano M, Yamahira T, Itai S, Jinno S, Kawahara H. Development of novel chitosan derivatives as micellar carriers of taxol. Pharm Res. 1998;15: 1844–1850.

[16]. Anitha A, Chennazhi KP, Nair SV, Jayakumar R. 5-florouracil loaded N,O-carboxymethyl chitosan nanoparticles as an anticancer nanomedicine for breast cancer. J Biomed Nanotech 2012; 8: 29-42.

[17]. Mi Z, Burke TG. Marked interspecies variations concerning the interactions of camptothecin with serum albumins: a frequency-domain fluorescence spectroscopic study. Biochem 1994; 33: 12540–12545.

[18]. Vinogradov SV, Bronich TK, Kabanov AV. Nanosize cationic hydrogels for drug delivery: preparation, properties and interaction with cells. Adv Drug Deliv Rev. 2002; 54: 135-147.

[19]. Owens III DE, Peppas NA. Opsonization, biodistribution, and phamacokinetics of polymeric nanoparticles. Int J Pharm. 2006; 307: 93-102.

[20]. Lemarchand C, Gref R, Couvreur P. Polysaccharide-decorated nanoparticles. Eur J Pharm Biopharm. 2004; 58: 327-341.

[21]. Brannon-Peppas L, Branchette JO. Nanoparticule and targeted systems for cancer therapy. Adv Drug Deliv Rev. 2004; 56: 1649-1659.

[22]. Muzzarelli RAA, Tonfani F, Emanuelli M, Mariotti S. N- (carboxymethylidene) chitosans and N-(carboxymethyl)-chitosan: novel chelating polyampholites obtained from chitosan glyoxylate. Carbohydr Res. 1982; 107: 199-214.

[23]. Miranda MES, Marcolla C, Rodrigues CA, Wilhelm HM, Sierakowski MR, Bresolin TMB, Freitas RA. Chitosan and N carboxymethylchitosan I: The role of N-carboxymethylation of chitosan in the thermal stability and dynamic mechanical properties of its films. Polym Int. 2006; 55: 961-969.

[24]. Lamim R, Freitas RA, Rudek EI, Wilhelm HM, Cavalcanti OA, Bresolin TMB. Films of chitosan and N-carboxymethylchitosan. Part II: Effect of plasticizers on their physiochemical properties. Polym Int. 2006; 55: 970-977.

[25]. Guinesi LS, Cavalheiro ETG. The use of DSC curves to determine the acetylation degree of chitin / chitosan samples. Thermochim Acta. 2006; 444: 128-133.

[26]. Hirai A, Odani H, Nakajima A. Determination of degree of deacetylation of chitosan by 1H NMR spectroscopy. Polym Bull. 1991; 26: 87-94.

[27]. Lavertu M, Xia Z, Serreqi AN, Berrada M, Rodrigues A, Wang D, Buschmann MD, Gupta A. A validated 1H NMR

method for determination of the degree of deacetylation of chitosan. J Pharm Biomed Anal. 2003; 32: 1149-1158.

[28]. Amiji MM. Pyrene fluorescence study of chitosan self-association in aqueous solution. Carbohydr Polym. 1995; 26: 211-213.

[29]. Granada A, Murakami FS, Sartori T, Lemos-Senna E, Silva MA. Development and validation of an HPLC method to quantify camptothecin in polymeric nanocapsule suspensions. J AOAC. 2008; Int 91: 551-556.

[30]. An NT, Thien DT, Dong NT, Dung PL. Water-soluble N-carboxymethylchitosan derivates: Preparation, characteristics and its application. Carbohydr Polym. 2009; 75: 489-497.

[31]. Lavertu M, Darras V, Bushmann MD. Kinetics and efficiency of chitosan reacetylation. Carbohydr Polym. 2012; 87: 1192-1198.

[32]. Philippovaa OE, Korchagina EV, Volkov EV, Smirnov VA, Khokhlov AR, Rinaudo M. Aggregation of some water-soluble derivatives of chitin in aqueous solutions: Role of the degree of acetylation and effect of hydrogen bond breaker. Carbohydr Polym. 2012; 87: 687–694.

[33]. Yan M, Li B, Zhao X. Determination of critical aggregation concentration and aggregation number of acid-soluble collagen from walleye pollock (Theragra chalcogramma) skin using the fluorescence probe pyrene. Food Chem. 2010; 122: 1333-1337.

[34]. Thomas CJ, Rahier NJ, Hecht SM. Camptothecin: current perspectives. Bioorg Med Chem. 2004; 12: 1585-1604.

[35]. Mu L, Elbayoumi TA, Torchilin VP. Mixed micelles made of poly (ethylene glycol)-phosphatidylethanolamine conjugate and D- -tocopheryl polyethylene glycol 1000 succinate as pharmaceutical nanocarriers for camptothecin. Inter J Pharm, 2005; 306: 142- 149.

[36]. Cortesi R, Esposito E, Maietti A, Menegatti E, Nastruzzi C. Formulation study for the antitumor drug camptothecin: liposomes, micellar solutions and a microemulsion. Int J Pharm. 1997; 159: 95-103.

[37]. Barreiro-Iglesias R, Bromberg L, Temchenko M, Alan-Hatton T, Concheiro A, Alvarez-Lorenzo C. Solubilization and stabilization of camptothecin in micellar solution of pluronic-g-poly (acrylic acid) copolymers. J Control Release. 2004; 97: 537-549.

[38]. Law D, Schimitt EA, Marsh KC, Everitt EA, Wang W, Fort JJ, Krill SL, Qiu Y. Ritonavir-PEG 8000 amorphous solid dispersions: In vitro and In vivo evaluations. J Pharm Sci. 2004; 93: 563-570, 2004.